SKB

Analysis of radiation damage in canister steel – project REBUS

Karin Andgren

SVENSK KÄRNBRÄNSLEHANTERING

Analysis of radiation damage in canister steel – project REBUS

Karin Andgren, Svensk Kärnbränslehantering AB

Preface

The reference design on which the licensing of the KBS 3 system for the management of spent nuclear fuel is based includes a reference canister for final disposal. The reference canister, which fulfils all established design requirements for post-closure safety, consists of an outer, corrosion resistant copper shell and a load-bearing nodular cast iron insert. In SKB's continuous efforts to optimise the design of the KBS-3 repository, it is evaluated whether an alternative design of the load-bearing insert can be achieved through a simpler and more cost effective production process. As an alternative to the reference nodular cast iron insert, a design with an outer low-alloy carbon steel tube and an inner framework of carbon steel plates for either 12 BWR or 4 PWR fuel elements is being studied in the so-called Rebus project. Within the project it is evaluated if such a design has the prospects of fulfilling the same design requirements as the reference canister insert, and if this can be achieved efficiently in a full-scale production process. The Rebus insert has the same outer dimensions as the reference insert and is intended to be placed in a copper shell identical to that of the reference design. The study documented in this report was performed to provide information that will help evaluate post-closure safety aspects of the proposed Rebus insert.

Abstract

Within the ongoing SKB project Rebus, SKB is re-evaluating the current reference design of the cast iron insert of the KBS-3 canister. Design alternative 1 (Concept 1) consists of a cylinder of carbon steel, with a carbon steel framework holding the fuel elements in place. Due to the differences in both material composition and geometry between the current insert and the design alternatives considered within the REBUS project, new calculations are performed of the radiation induced material damage (dpa/y) in steel. In addition, results for radiation dose to materials from neutron irradiation are presented.

Sammanfattning

Inom det pågående SKB-projektet Rebus görs en omvärdering av gjutjärnsinsatsen i KBS-3-kapseln. Designalternativ 1 består av en kolstålscylinder med en fackverkskonstruktion för att hålla bränsle-elementen. På grund av skillnader i material och konstruktion jämfört med referensdesignen, har nya beräkningar av dpa/år utförts. Även resultat för materialdos till följd av neutronstrålning presenteras.

Contents

1   Introduction

Within the ongoing SKB project Rebus, SKB is re-evaluating the current reference design (SKB 2010) of the cast iron insert of the KBS-3 canister. Design alternative 1 (Concept 1) consists of a cylinder of carbon steel, with a carbon steel framework holding the fuel elements in place (Ronneteg 2023).

Due to the differences in both material composition and geometry between the current insert and the design alternative 1 considered within the Rebus project, new calculations of the radiation fields extending from the encapsulated nuclear fuel and through the canister materials have been performed (Loberg 2023). Most results presented in Loberg (2023) are determined using a model with bentonite surrounding the canister, since this corresponds to the situation in the repository. The exception being determination of the dose to a person 2 m away from the canister, where air is assumed between the person and the canister. Only the model with bentonite is used for the results presented here. Particle fluxes are used to estimate the displacements per atom (dpa) per year, which can be used to quantify radiation damage in the canister's steel material. The dpa result also forms a crucial input to calculations of the formation of clusters of Cu atoms emanating from Cu impurities in the steel. For the repository model with bentonite surrounding the canister, the results presented by Loberg (2023) only showed gamma dose rates to materials since this is several orders of magnitude larger than the neutron dose rates. However, the neutron dose rates are also relevant for evaluating the evolution of the canister properties and therefore also neutron dose rates to material is presented here.

1.1   Basis for dpa calculations

The deliverables for this report are:

* Rate of displacements per atom from neutron radiation (dpa/y) in steel
* Rate of displacements per atom from gamma radiation (dpa/y) in steel
* Neutron dose rate to materials (Gy/h) in steel and Cu

For these calculations source terms corresponding to decay times 20, 50, 100, 1 000, 10 000, 100 000 and 1 000 000 years after encapsulation are used. Encapsulation is assumed to take place after 20 years of cooling (same as in Loberg 2023).

2 Computational method

Loberg (2023) used the code MCNP6.2 (Werner et al. 2018), and this version is also used for the purposes of the current report. Determination of dpa in steel is done for the positions A and B as specified in Loberg (2023). The positions are not always marked in the same spots in Loberg (2023) as where the material dose rate is actually determined, according to the MCNP calculations. The geometrical distribution for the volume tally used for determining the material dose from gamma in the calculations described in Loberg (2023) are:

- BWR position A
  - X: 9 cm [8 cm – 10 cm]
  - Y: 1.3 cm [0.8 cm – 1.8 cm]
  - Z: 22 cm – 90 cm

- BWR position B
  - R: 39.1 cm [39.05 cm – 39.15 cm]
  - Z: 22 cm – 112 cm
  - θ^1: 0.75 (revolutions) – 1 (revolutions)

- PWR position A
  - X: 16.5 cm [16 cm – 17 cm]
  - Y: 4.5 cm [4 cm – 5 cm]
  - Z: 97 cm – 107 cm

- PWR position B
  - R: 39.1 cm [39.05 cm – 39.15 cm]
  - Z: 97 cm – 107 cm
  - θ: 0.903 (revolutions) [0.900 (revolutions) – 0.906 (revolutions)]

The coordinates used for determining the material dose from neutrons in the calculations described in Loberg (2023) are:

- BWR position A
  - X: 6 cm [5 cm – 7 cm]
  - Y: 0.9 cm [0.8 cm – 1 cm]
  - Z: 0 cm – 60 cm

- BWR position B
  - R: 39.1 cm [39.05 cm – 39.15 cm]
  - Z: 0 cm – 60 cm
  - θ^2: 0.75 (revolutions) – 1 (revolutions)

- PWR position A
  - X: 8 cm [6.5 cm – 9.5 cm]
  - Y: 4 cm [3 cm – 5 cm]
  - Z: 10 cm – 60 cm

- PWR position B
  - R: 39.1 cm [39.05 cm – 39.15 cm]
  - Z: 10 cm – 70 cm
  - θ: 0.845 (revolutions) [0.82 (revolutions) – 0.87 (revolutions)]

---

[1] The absorbed dose is determined as an average over the entire 270° – 360° azimuthal angle in MCNP. Resulting value is then multiplied with the form factor 1.6 corresponding to 0.95 revolutions or 342°.

[2] The absorbed dose is determined as an average over the entire 270° – 360° azimuthal angle in MCNP. Resulting value is then multiplied with the form factor 1.03 corresponding to 0.95 revolutions or 342°.

where X, Y, R = 0 is located at the centre of the canister and θ is the reference angle for the cylindrical mesh tally as specified in Figure 2-1. Z = 0 is located at the mid-height of the fuel rod. One revolution corresponds to 360° and 0.75 revolutions correspond to 270° in the Loberg model. This means that e.g. 0.903 revolution correspond to 325° and 0.845 revolutions corresponds to 304°. Cross sections as function of particle energy for energy deposition and dpa are not identical. This means that the positions where the maximum dose rate is reached are not necessarily the same as the positions for maximum dpa rate. The positions in the horizontal plane as defined above are shown in Figure 2-1 and Figure 2-2. Positions in the Z-direction differ slightly for different positions (see above). Positions C and D are also marked in the figures, the C and D positions for neutron transport are described in Section 3.3.
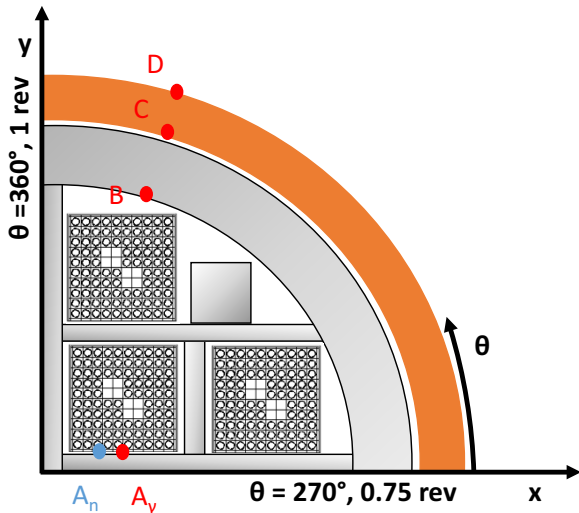

Figure 2-1. *Positions A-D where the material dose rate and/or fluxes are determined for the BWR canister. Position A is different depending on particle (gamma or neutron).*
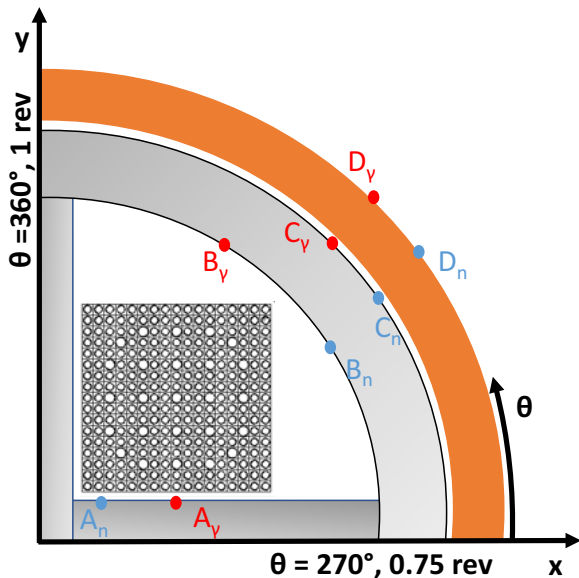

Figure 2-2. *Positions A-D where the material dose rate and/or fluxes are determined for the PWR canister. The positions are different depending on particle (gamma or neutron).*

The displacement rate, R_D, is described by Toijer (2014) as:

$$R_D = \int_{\check{E}}^{\hat{E}} \phi\,(E_i)\,\sigma_D(E_i)\,dE_i$$

Results for neutrons are determined using Fispact (Sublet et al. 2015, pp 125–126) with the neutron flux and material composition as described in Loberg (2023). Results for gamma irradiation are determined using damage cross-sections, σ_D, as described in Toijer (2014) together with electron flux, ϕ, given by the MCNP-model described in Loberg (2023). The input files to the MCNP-model and the Fispact calculations, as well as the script used to determine the dpa cross sections, are stored at SKB (svn://svn.skb.se/RS/RSK/).

2.1   Gamma damage

The displacement cross-section for scattering of electrons, $\sigma_D(E_i)$, with kinetic energy E_i is given by Toijer (2014):

$$\sigma_D(E_i) = \int_0^\pi \frac{d\sigma_{Born}}{d\Omega}\,2\pi \sin\theta\,v(E_i, \theta)\,d\theta$$

where θ is the scattering angle and the scattering cross-section is given by Fernández-Varea et al. (1993):

$$\frac{d\sigma_{Born}}{d\Omega} = \frac{(2m_e\gamma Ze^2)^2}{q^4}[1 - F_e(q)]^2$$

where m_e is the rest mass of the electron, $\gamma = E_i/(m_ec^2)+1$ is the Lorentz factor, $q = 2p \sin \theta/2$ in which $p = \gamma\beta m_ec$. The screening function, $F_e(q)$, goes to zero for low energies and needs not to be accounted for according to Toijer (2014). The cross-section used here is then:

$$\frac{d\sigma_{Born}}{d\Omega} = \frac{(2m_e\gamma Ze^2)^2}{(4\pi\epsilon_0)^2 q^4}$$

where the Coulomb constant of $4\pi\epsilon_0$ is added explicitly in the denominator.[3] The number of displaced atoms, $v(E_i,\theta)$, resulting from a primary knock-on atom (PKA) of mass M with energy T, transferred from the electron

$$T = \frac{2E_i}{Mc^2}(E_i + 2m_ec^2)\,\sin^2\left(\frac{\theta}{2}\right)$$

is approximated by the modified Kinchin and Pease model (Toijer 2014):

$$v(T) = \begin{cases} 0 & \text{for } T < E_{min} \\ T/E_d & \text{for } E_{min} < T < E_d \\ 1 & \text{for } E_d < T < 2\,E_d \\ \dfrac{T}{2E_d} & \text{for } 2E_d < T < E_c \end{cases}$$

where E_{min} = 15 eV, E_d = 40 eV (Toijer 2014) and E_c is the cut-off energy for electron stopping, which can be determined using E_c (keV) = M (amu) = 55.8e3 eV. The mass of iron atoms is used since iron composes 97.5 w-% of the steel insert (a similar percentage is valid also for the cast iron in the reference canister). The transferred energy does not exceed E_c for the gamma source term from spent nuclear fuel. The displacement cross-section for different incoming electron energies was determined using a left Riemann sum with θ from 0 to π and a step of 1e−5. Results are presented in Table 2-1.

---

[3] Toijer (2014) is using a factor of $8\pi\epsilon_0$ instead, which means that the cross-sections presented here are higher than the ones used by Toijer (2014).

Table 2-1. Displacement cross-section, σ_D, for different electron energies E_i.

E_i (keV)	σ_D (barn)
111	0
200	0
300	1.23
400	23.4
500	38.1
600	49.2
700	57.7
821	64.3
1 350	77.8
2 230	92.5

The determined cross-sections are similar to the ones presented in figure 15 in Oen (1965). The MCNP calculations for gamma transport were adjusted to include transport of electrons and the cross-sections where applied in MCNP using the DE and DF cards for point wise multiplication with the electron fluxes. Linear interpolation was applied for electron energies between values in the table. Electron fluxes as determined by MCNP are shown in Table 2-2. As can be seen from Table 2-1 the cross-section for electron energies below 200 keV is zero. Electron fluxes below 100 keV were therefore not determined for the PWR insert.

Table 2-2. Binned electron flux (e/cm²s) at position A and B for the BWR and the PWR insert at encapsulation (y=0).

E_i (keV)	E_i (keV)	BWR		PWR	
Upper	Lower	Pos. A	Pos. B	Pos. A	Pos. B
[1]2.23e3	1.35e3	9.30e3	1.68e4	1.25e4	8.92e3
1.35e3	8.21e2	3.28e5	3.29e5	4.58e5	3.64e5
8.21e2	5.0e2	1.79e6	1.44e6	2.11e6	1.99e6
5.0e2	1.11e2	4.84e7	4.08e7	6.06e7	5.89e7
1.11e2	9.12e0	2.78e7	2.15e7	3.81e6	3.42e6
9.12e0	5.53e0	6.79e5	5.31e5	N.A.[2]	N.A.[2]
5.53e0	1.49e−1	1.06e6	8.33e5	N.A.[2]	N.A.[2]

[1] Results in this energy group has poor statistics with relative errors > 0.1
[2] Electron fluxes for energies below 100 keV were not determined for the PWR insert.

2.2 Neutron damage

The neutron flux at position A and B, Table 3-14 and 3-15 in Loberg (2023) for BWR and Table 3-6 and 3-7 in Loberg (2023) for PWR, were used in Fispact (Sublet et al. 2015) with the cross-section library TENDL-2017 to determine the total displacement rate. The material composition was specified using data of the MCNP model (Loberg 2023). Since the source neutron spectrum is independent of decay time, the neutron spectra at the different positions will also be independent of decay time. The spectrum for decay time 0 y is therefore used multiplied with the flux ratio of the decay time of interest according to Table 2-1 in Loberg (2023).

2.3 Neutron dose to materials

Doses to materials from gamma radiation are presented in Loberg (2023). Results from neutron irradiation are presented here. MCNP presents the dose in MeV/cm³ and the results are converted to J/kg (or Gy) by multiplying with 1.60218e−13 J/MeV and dividing by 7.8e−3 kg/cm³ (the same steel density as used in the MCNP-files of Loberg (2023), however final results as presented in Loberg (2023) are determined using a steel density of 7.95 kg/cm³. Source particles per hour are determined using Table 2-1 in Loberg (2023).

3 Results

3.1 Dpa per year

Results from neutron irradiation are presented up to 1 000 000 years after encapsulation.

Table 3-1. Dpa/y from neutron irradiation at position A and B for the BWR and the PWR insert.

	BWR 50 MWd/kgU	BWR 50 MWd/kgU	PWR 55 MWd/kgU	PWR 55 MWd/kgU
Years after encap.	Pos. A (dpa/year)	Pos. B (dpa/year)	Pos. A (dpa/year)	Pos. B (dpa/year)
20	1.13e−9	5.73e−10	1.04e−9	7.62e−10
50	4.08e−10	2.06e−10	3.83e−10	2.80e−10
100	1.20e−10	6.06e−11	1.18e−10	8.67e−11
1 000	6.19e−11	3.13e−11	4.99e−11	3.65e−11
1e4	2.26e−11	1.14e−11	1.78e−11	1.30e−11
1e5	5.63e−12	2.85e−12	4.43e−12	3.25e−12
1e6	1.09e−12	5.50e−13	8.91e−13	6.53e−13

Results from gamma irradiation are presented up to 1 000 years after encapsulation. The dpa/y from gamma is less than 1% of the dpa/y from neutrons at this time. It is therefore not necessary to determine the damage rate from gamma for longer times than 1 000 years after encapsulation.

Table 3-2. Dpa/y from gamma irradiation at position A and B for the BWR and the PWR insert.

	BWR 50 MWd/kgU	BWR 50 MWd/kgU	PWR 55 MWd/kgU	PWR 55 MWd/kgU
Years after encap.	Pos. A (dpa/year)	Pos. B (dpa/year)	Pos. A (dpa/year)	Pos. B (dpa/year)
20	5.58e−9	4.89e−9	7.11e−9	6.94e−9
50	2.77e−9	2.43e−9	3.53e−9	3.44e−9
100	8.70e−10	7.63e−10	1.11e−9	1.08e−9
1 000	2.89e−13	2.53e−13	1.02e−13	9.98e−14

The summed dpa/s, $G(t)$, at position A for the BWR insert can be described using the following equation:

$$G(t) = ae^{-bt} + \frac{c}{\sqrt{t}}$$

where t is the time after encapsulation in seconds and the parameters a, b and c are found by least-squares fitting:

- $a = 3.520e{-}16$
- $b = 7.886e{-}10$
- $c = 1e{-}12.45$

The results presented in the tables above and results using the expression $G(t)$ are shown in Figure 3-1.
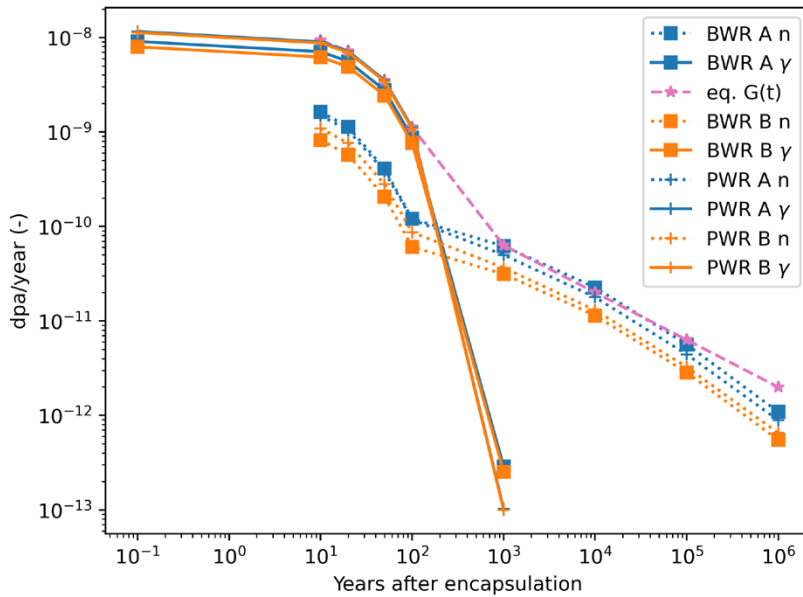
Figure 3 -1. *Dpa per year from neutrons and gamma for positions A and B of the BWR and PWR inserts. Results using the empirical expression G(t) are also shown.*

3.2 Accumulated dpa from neutrons

The accumulated dpa after 100 000 y for neutrons can be determined by integrating over the values in Table 3-1. The middle Riemann sum over the values in Table 3-1 are presented in Table 3-3.

Table 3-3. Accumulated dpa from neutron irradiation after 100 000 y.

	BWR 50 MWd/kgU	BWR 50 MWd/kgU	PWR 55 MWd/kgU	PWR 55 MWd/kgU
Years after encap.	Pos. A (dpa)	Pos. B (dpa)	Pos. A (dpa)	Pos. B (dpa)
1e5	9.85e–7	4.97e–7	7.93e–7	5.79e–7

The obtained dpa can be compared to previous results presented in Table 3-2 in Yang et al. (2019).

Table 3-4. Comparison of results at position D as defined in Yang et al. (2019) for a PWR canister and position B of this work.

	Yang et al. (2019)	This work
	PWR [1]50 MWd/kgU Pos. D	PWR 55 MWd/kgU Pos. B
Dpa/year	9.59e–10	~[2]5e–10
Dpa after 1e5 years	1.17e–6	5.79e–7

[1] Burn-up is most likely 50 MWd/kgU, however the traceability of this figure is poor.
[2] Logarithmic interpolation between 20 y and 50 y.

Both the dpa/y 30 years after encapsulation and the accumulated dpa after 100 000 years is about a factor two less than the previous value presented in Yang et al. (2019).

3.3 Dose rate to steel from neutrons

Dose rate to steel from neutrons are determined for positions A and B as specified in chapter 2. Dose rates were also determined for positions C and D (as specified in Loberg 2023), corresponding to R = 47.85 cm [47.6 cm – 48.1 cm] (C) and R = 52.25 cm [52.0 cm – 52.5 cm] (D) for both PWR and BWR. Values for Z and θ are the same as for position B. Resulting dose rates are presented in Table 3-5, Table 3-6 and Figure 3-2.

Table 3-5. Neutron dose rates for the BWR canister, positions A–D for different years after encapsulation.

Years after encap.	A (Gy/h)	B (Gy/h)	C (Gy/h)	D (Gy/h)
0	2.15e−4	1.15e−4	8.70e−5	3.27e−4
20	1.04e−4	5.53e−5	4.20e−5	1.58e−4
50	3.73e−5	1.99e−5	1.51e−5	5.68e−5
100	1.10e−5	5.86e−6	4.45e−6	1.67e−5
1 000	5.67e−6	3.02e−6	2.29e−6	8.63e−6
1e4	2.07e−6	1.10e−6	8.38e−7	3.15e−6
1e5	5.16e−7	2.75e−7	2.09e−7	7.85e−7
1e6	9.96e−8	5.31e−8	4.03e−8	1.52e−7

Table 3-6. Neutron dose rates for the PWR canister, positions A–D for different years after encapsulation.

Years after encap.	A (Gy/h)	B (Gy/h)	C (Gy/h)	D (Gy/h)
0	1.95e−4	1.67e−4	1.43e−4	3.68e−4
20	9.44e−5	8.08e−5	6.95e−5	1.79e−4
50	3.47e−5	2.97e−5	2.56e−5	6.57e−5
100	1.07e−5	9.19e−6	7.91e−6	2.03e−5
1 000	4.53e−6	3.87e−6	3.33e−6	8.56e−6
1e4	1.61e−6	1.38e−6	1.19e−6	3.05e−6
1e5	4.03e−7	3.44e−7	2.96e−7	7.61e−7
1e6	8.09e−8	6.93e−8	5.96e−8	1.53e−7

The bentonite outside the canister acts as a neutron reflector and the dose rate is therefore highest at position D for both the BWR and the PWR canister.
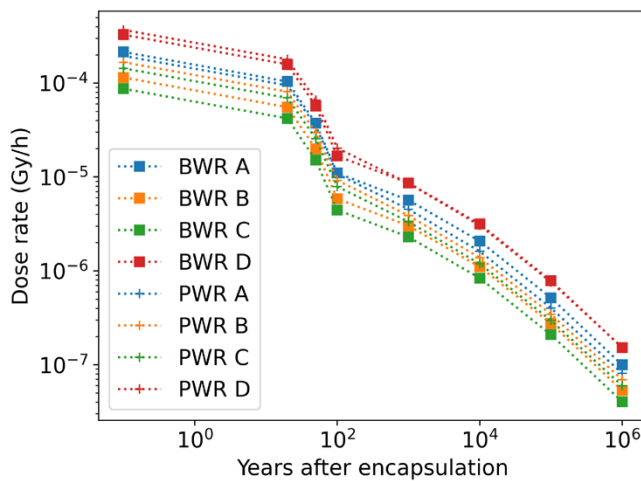

Figure 3-2. *Neutron dose rate for positions A-D for the BWR and PWR canisters at different times after encapsulation.*

References

SKB's (Svensk Kärnbränslehantering AB) publications can be found at www.skb.com/publications. SKBdoc documents will be submitted upon request to document@skb.se.

Fernández-Varea J M, Mayol R and Salvat F, 1993. Cross sections for elastic scattering of fast electrons and positrons by atoms. Nuclear Instruments and Methods in Physics Research Section B: Beam Interactions with Materials and Atoms 82:1, 39-45.

Loberg J, 2023. Dose rate calculations – project REBUS. SKB R-22-08, Svensk Kärnbränslehantering AB.

Oen O S, 1965. Cross sections for atomic displacements in solids by fast electrons. Nuclear Instruments and Methods in Physics Research Section B: Beam Interactions with Materials and Atoms 33:1–4, 744–747.

Ronneteg U, 2023. Version 4.0 av 1939700 KBP3021 REBUS – Input parameters post-closure safety – Concept 1. SKBdoc 2026552 ver 1.0, Svensk Kärnbränslehantering AB.

SKB, 2010. Design, production and initial state of the canister. SKB TR-10-14, Svensk Kärnbränslehantering AB.

Sublet J-C C, Eastwood J W, Morgan J G, Fleming M, Gilbert M R (eds), 2015. The FISPACT-II user manual. UKAEA Report UKAEA-R (11)11 Issue 7, UK Atomic Energy Authority.

Toijer E, 2014. Assessment of primary damage and copper precipitation in cast iron in repository conditions. Master's thesis. Royal Institute of Technology, Sweden.

Werner C J, Bull J S, Solomon C J, Brown F B, McKinney G W, Rising M E, Dixon D A, Martz R L, Hughes H G, Cox L J, Zukaitis A J, Armstrong J C, Foster Ill R A, Caswell L, 2018. MCNP6.2 Release Notes. Report LA-UR-18-20808, Los Alamos National Laboratory, USA.

Yang Q, Toijer E, Olsson P, 2019. Analysis of radiation damage in the KBS-3 canister materials. SKB TR-19-14, Svensk Kärnbränslehantering AB.

SKB is responsible for managing spent nuclear fuel and radioactive waste produced by the Swedish nuclear power plants such that man and the environment are protected in the near and distant future.

skb.se